BMC Genomics

RESEARCH Open Access

Genomic alterations of marine yeast *Scheffersomyces spartinae* under spontaneous and mutagenic conditions

Yu-Ting Bai[1,2†], Awkash Sharma[2†], Qian Xiang[2], Li-Yan Tian[2], Ke-Jing Li[2], Bao-Ying Guo[1], Lei Qi[2,3*] and Dao-Qiong Zheng[1,2]

Abstract

Background Understanding the mechanisms of genetic evolution in marine yeasts is essential for their ecological and biotechnological applications. *Scheffersomyces spartinae*, an ascomycetous yeast species, characterized by its remarkable robustness and carbon source utilization capability, has garnered significant attention for its biotechnological potential.

Results In this study, we investigated the spontaneous and induced genomic alterations of the marine yeast *S. spartinae* under various conditions. Through mutation accumulation experiments combined with whole-genome sequencing, we revealed that the rates of spontaneous single nucleotide variations and small insertions and deletions were 6.3×10^{-11} and 1.4×10^{-11} per base pair per cell division, respectively, in *S. spartinae*. The predominant type of base substitution was C-to-T or G-to-A, likely induced by cytosine deamination. Template slippage during DNA replication emerged as the primary cause of small InDels. 50 J/m^2 UV treatment elevated the SNV rate by 124-fold, with C-to-T substitutions occurring at the 5′-TC-3′ motif and T-to-C substitutions at the 5′-TT-3′ motif being the most prominent features. Exposure to 50 μg/mL Zeocin resulted in 76-fold and 71-fold increases in the rates of SNVs and InDels, respectively, with frequent T-to-A mutations and T deletions occurring at the 5′-GT-3′ motifs. Heat stress at 37 °C increased the SNVs and InDels rates to 1.4×10^{-10} and 7.5×10^{-11} per base pair per cell division. Notably, this study demonstrated that large deletions and duplications (> 1 kb) and aneuploidies are less likely to occur in *S. spartinae* compared to other yeast species, suggesting that this organism is less tolerant to large-scale genomic alterations. In contrast, we observed a marked decrease in rDNA copy numbers when *S. spartinae* cells were cultivated at elevated temperature conditions. This finding indicates that variations in rDNA copy numbers might act as an adaptive strategy for yeasts in response to fluctuating temperatures.

Conclusions Our findings provide novel insights into the patterns and genetic mechanisms underlying genomic evolution in yeasts.

Keywords Marine yeast, Mutagen, DNA mutation, rDNA copy number, High temperature

†Yu-Ting Bai and Awkash Sharma contributed equally to this work.

*Correspondence:
Lei Qi
qilei0917@zju.edu.cn

[1]Marine Science and Technology College, Zhejiang Ocean University, Zhoushan 316021, China
[2]Ocean College, Zhejiang University, Zhoushan 316021, China
[3]Department of Molecular Genetics and Microbiology, Duke University, Durham 27710, USA

Background

Yeasts are single-celled eukaryotes that serve as valuable models for biological studies and as cell factories for various industrial applications. Among them, *Saccharomyces cerevisiae* is the most widely used yeast in genetics and biotechnology [1, 2]. Recently, certain yeasts from marine environments have garnered increased attention due to their unique physiological and phenotypic traits [3, 4]. For instance, the oleaginous yeast *Yarrowia lipolytica* can thrive in diverse habitats such as soil, sewage, and oil-contaminated sites [5]. Additionally, it possesses the remarkable ability to assimilate a broad spectrum of both hydrophobic and hydrophilic carbon sources [6, 7]. The yeast *Scheffersomyces spartinae* exhibits high salt resistance, the ability to utilize multiple carbon sources, and shows potential for applications such as coenzyme Q9 production and azo dye degradation [8, 9]. A recent study provided a telomere-to-telomere assembly of the *S. spartinae* genome, revealing abundant genetic variations between different strains of this species [10]. However, the underlying mechanisms behind these variations remain poorly understood.

Genomic alterations are fundamental sources of genetic diversity and phenotypic evolution in organisms, encompassing a wide range of changes in DNA sequences and structures. These alterations include single nucleotide variations (SNVs), small insertions and deletions (InDels), chromosomal rearrangements (such as large deletions and duplications), loss of heterozygosity (LOH; gene conversion and crossover), and whole-chromosome aneuploidy [11]. Such changes can occur spontaneously or be induced by stressors, including DNA-damaging agents like ultraviolet (UV) light and methylmethane sulfonate, which are widely used as mutagens in genetic and breeding studies [12]. Therefore, investigating the patterns and mechanisms of genomic alterations under both spontaneous and stress-induced conditions is crucial for elucidating their roles in phenotypic evolution and for developing innovative strategies to construct robust strains.

Traditionally, yeast reporter genes such as *URA3* and *CAN1*, whose dysfunction results in selectable phenotypes, have been widely used to detect DNA mutation frequencies and spectra [11]. With the development of high-throughput sequencing technology, yeast strains subjected to mutation accumulation (MA) experiments followed by whole-genome sequencing have proven to be powerful tools for analyzing genomic alterations [13–15]. Using this strategy, Sui et al. found that the rates of SNVs, small InDels, LOH, and large-scale chromosomal rearrangements in the diploid *S. cerevisiae* strain were 4.8×10^{-3}, 2.7×10^{-4}, 4.7×10^{-3}, and 1.8×10^{-3} events per genome per cell division, respectively [15]. Furthermore, their data revealed that these genetic events were non-randomly distributed across the chromosomes. Exposure to UV [16–18], phleomycin (Zeocin) [19, 20], high temperature [21], hydrogen peroxide [22], and furan derivatives [23–25] has led to increased rates of certain genomic alterations and modified their patterns as well. For instance, our previous work found that exposure to Zeocin resulted in an increase in SNVs and InDels by two orders of magnitude in *S. cerevisiae*, with T-to-G being the most prominent base substitutions [20]. Although multiple studies have been conducted to reveal genetic modifications under various conditions in *S. cerevisiae*, it remains unclear whether the inference obtained from this model yeast can be applied to other non-classical yeasts, including the wild-type marine yeast *S. spartinae*.

In this study, we investigated spontaneous and physical/chemical factor-induced genomic alterations in *S. spartinae* using MA experiments combined with next-generation whole-genome sequencing. Our findings revealed that UV radiation, Zeocin, and heat stress resulted in distinctly different DNA mutation spectra within the *S. spartinae* genome. We further examined the variations in genomic alteration patterns between *S. spartinae* and *S. cerevisiae*, discussing potential underlying genetic mechanisms. These results provide new insights into the genetic mechanisms driving genomic evolution in yeasts.

Materials and methods

Yeast strains and growth conditions

The marine yeast *S. spartinae* YMxiao (CCTCC AY 2022004), was originally isolated from the sea water of Dongji Island in Zhoushan city, China [10]. YPD medium, which consisted of 1% (w/v) yeast extract, 2% (w/v) peptone, and 2% (w/v) dextrose, was used to culture this strain. Incubation was carried out at 30 °C or an indicative temperature.

MA experiment of *S. spartinae* Ymxiao

To investigate spontaneous genomic alterations in the diploid marine yeast *S. spartinae*, we subcultured 19 independent MA lines (isolates) of YMxiao on solid YPD medium for either 60 (10 isolates) or 100 (9 isolates) generations. During each subculture cycle, we randomly selected one colony from a YPD plate and streaked a single colony onto a new YPD plate for each MA line. The cells subcultured on YPD plates and incubated at 30 °C for 2 days for each generation. For UV radiation exposure, 5 MA lines of YMxiao were exposed to 254 nm UV light at an intensity of 50 J/m² using a UV crosslinker (UVP CL-1000) after streaking for 90 s, followed by incubation at 30 °C for 2 days. For Zeocin treatment, 9 MA lines of YMxiao were stroke on YPD plates containing 50 μg/mL Zeocin (InvivoGen) and then incubated at 30 °C for 3 days. The MA lines treated with

UV and Zeocin treatment were subcultured for 10 generations. To explore heat-induced genomic alterations, 21 MA lines of YMxiao were incubated on YPD plates at 37 °C for 30 (3 isolates), 60 (13 isolates), or 90 (5 isolates) generations. We sequenced several isolates after 30 generations of subculture under 37 °C. Whole genome sequencing was then performed to detect genetic events in the subcultured isolates under above mentioned conditions (Fig. 1A).

Genome sequencing of *S. spartinae* isolates

The genomic DNA (gDNA) of yeast cells were extracted using the Genomic DNA extraction kit (Apostle MiniGenomics), and the quality of the gDNA is assessed using the Qubit dsDNA BR Assay Kit 501 assays (Invitrogen) and gel electrophoresis. Subsequently, index adapters are added to the gDNA using Adapter Set 8 for MGI (Vazyme), and the VAHTS® Universal Plus DNA Library Prep Kit for MGI (Vazyme) is used to construct the library on the MGISP-960(MGI), with subsequent quality control of the library. The library is then circularized using the VAHTS® Vircularization Kit for MGI (Vazyme), and the genomic DNA is sequenced on the MGISEQ-2000(MGI)sequencer using a 2 × 150 bp paired-end indexing scheme. Raw sequencing reads were quality-checked using FastQC (v0.11.9) and trimmed with Trimmomatic (v0.39) to remove low-quality bases (Phred score < 20) and adapter sequences.

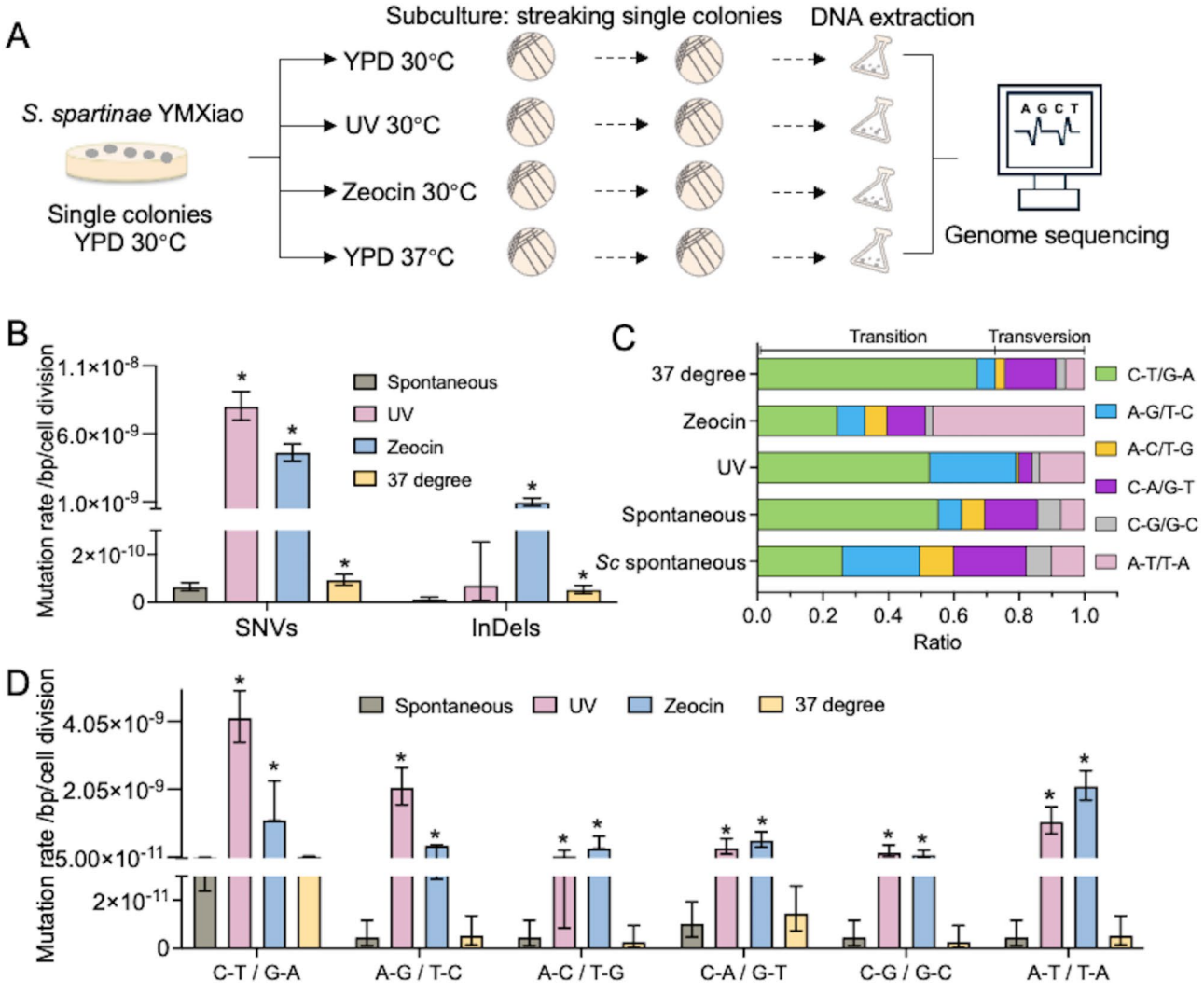

Fig. 1 Distinct rates and spectrum of spontaneous and induced point mutations. (**A**) Mutation accumulation method. To induce genomic alterations, isolates of *S. spartinae* YMxiao were repeatedly subcultured on solid medium under specific conditions. During each cycle, YMxiao cells were streaked onto the solid medium to isolate single colonies. After completing mutation accumulation, the cells were expanded through large-scale cultivation and subjected to Illumina whole genome sequencing. (**B**) The rates of SNVs and InDels under various conditions. (**C**) Ratios of 6 types of base substitutions (transitions and transversions) in *S. spartinae* isolates. (**D**) The rate of each individual base substitution. The data are shown as the means ± SD. *P*-values were determined using the Wilcoxon rank-sum test and $P < 0.05$ are indicated with asterisks

Detection of SNVs and indels

High-quality reads were aligned to the *S. spartinae* YMxiao reference genome using BWA-MEM algorithm (v0.7.17) with default parameters [26]. The output sam files were converted to bam files and sorted using SAMtools (v1.10). SNPs and InDels were identified using VarScan (v2.4.3). The resulting Variant call format (VCF) files were filtered to exclude low-confidence variants using standard hard filters: base quality ≥ 30, mapping quality ≥ 40, and strand bias *p*-value ≥ 0.05. Variants were annotated using SnpEff (v4.3) with the pre-annotated *S. spartinae* YMxiao genome database to predict their impact on coding sequences and regulatory regions.

Mutation rates μ_{bp} per base pair per cell division were calculated as follows: $\mu_{bp} = \frac{n_{bp}}{N \times gen_{tot} \times t}$, where nbp is the number of mutations of any type of SNVs or InDels, *N* is 24,000,000 (the number of base pairs of the diploid genome of *S. spartinae* YMxiao), gen_{tot} is the total number of subculture generations, and t is the number of cell divisions from a cell to form a colony.

Analysis of DNA copy number variations

The sequencing coverage of each base of the genomes of *S. spartinae* isolates were calculated by bedtools, using the sorted BAM files as inputs [27]. The depth of coverage for each sample was calculated using with a bin size of 2000 bp and a sliding step of 1000 bp using a custom python script (Supplemental text). The coverage information was further used for graphical representation using a custom R script (Supplemental text). To calculate the copy numbers of rDNA repeats (located between 836,000 and 897,000 on chr H), the "depth" algorithm of samtools was used as: samtools depth -r chrG:836,000-897,000 sample.bam| awk '{sum+=$3} END {if (NR > 0) print sum/NR}'.

Statistical analysis

The 95% confidence interval of mutation rates were modeled using a Poisson distribution. To evaluate the statistical significance of differences in mutation rates between the YPD control and stressful conditions, Wilcoxon rank-sum test was performed, with a *P* value of less than 0.05 considered statistically significant.

Results

Spontaneous genomic alterations in the marine yeast *S. spartinae*

Mapping the sequencing reads to the reference genome of *S. spartinae* revealed a total of 56 SNVs across 19 isolates subcultured under spontaneous conditions (10 isolates for 60 generations and 9 isolates for 100 generations) (Dataset S1). During the two-day growth period on solid YPD medium, each isolate underwent approximately 25 cell divisions per generation. This resulted in a total of 385,500 cell divisions, calculated as follows: $9 \times 25 \times 60 + 10 \times 25 \times 100 = 385{,}500$, where 9 and 10 represent the number of isolates, 60 and 100 represent the number of generations, and 25 represents the number of cell divisions per generation. Similar to observations in *S. cerevisiae* [15], the mutation rate remained constant throughout the long-term MA experiment, with no significant differences in mutation rates between strains from 60 to 100 generations (Dataset S1). Consequently, the occurrence of SNVs in the *S. spartinae* genome was estimated at 56/385,500, equating to 1.5×10^{-3} SNVs per cell division. Considering the genome size of YMxiao is approximately 11.5 Mb (excluding repetitive regions), we further calculated the SNV rate to be 6.3×10^{-11} per base per cell division (Fig. 1B). Among the six types of base substitutions identified, C-to-T and G-to-A transitions constituted the majority at 55%, which is higher than that in *S. cerevisiae* (Fig. 1C and D). Additionally, the ratio of transitions (CG-to-TA and TA-to-CG) was found to be 1.7-fold higher than that of the four types of transversions (CG-to-AT, TA-to-GC, CG-to-GC, and TA-to-AT, Fig. 1C). Of the 56 SNVs detected, 45 occurred in protein-coding regions, including 31 missense variants and 14 synonymous variants (Supplemental Dataset S1). The relative ratio of intergenic and intragenic SNVs aligned well with the lengths of intergenic (8.5 Mb) and intragenic (3.9 Mb) regions.

We also identified 11 InDels (7 deletions and 4 insertions) through genome sequencing, resulting in an InDels rate of 1.2×10^{-11} per base pair per cell division (Fig. 1B and Dataset S1). The sizes of these InDels ranged from 1 bp to 6 bp. By analyzing the adjacent sequences, we found that all of these InDels occurred in DNA regions characterized by short tandem repeats, such as (T)n, (AT)n, and (TCT)n (Fig. 2A). This observation suggests that DNA replication slippage is the primary mechanism underlying InDels during spontaneous cell division (Fig. 2B). Notably, although intergenic regions comprise only 29% of the *S. spartinae* genome, 7 out of the 9 InDels were located within these intergenic regions (Supplemental Dataset S1). Strikingly, we discovered that more than 90% of the SNVs and InDels were homozygous between the two homologs of the diploid *S. spartinae* genome (Supplemental Dataset S1), indicating that these mutations had undergone purification driven by chromosomal recombination. In *S. cerevisiae* strains defective in meiosis, most (> 95%) point mutations occurring during the subculture process were heterozygous, as the frequency of mitotic DNA recombination is low. Therefore, the mutation purification phenomenon observed in *S. spartinae* isolates is likely driven primarily by meiotic chromosome crossovers.

Fig. 2 Spontaneous InDels and possible genetic mechanisms. (**A**) The 11 InDels identified in the isolates subcultured under spontaneous conditions. The underlined bases indicate deletions, while the triangles represent insertions. The blue bases indicate short repeats. (**B**) Illustrations of tandem repeats that facilitate template slippage during DNA replication, leading to small deletions or duplications

By analyzing the sequencing coverage of the YMxiao isolates, we did not detect any large deletions and duplications greater than 1 kb or aneuploidy events. Assuming that at least one deletion/duplication or aneuploidy event occurred among the 19 subcultured isolates, we estimated the rate of such genetic event to be 2.6×10^{-5} per genome per cell division. This rate is notably lower than the 1.8×10^{-4} events per genome per cell division observed in a diploid *S. cerevisiae* strain [15].

UV induced genomic alterations in *S. spartinae*

UV radiation is a well-known environmental mutagen capable of causing significant DNA damage and is widely utilized in microbial genetic breeding [16, 28]. The most common mutation induced by UV light is the formation of pyrimidine dimers, particularly thymine dimers [29]. These dimers distort the DNA helix, hindering accurate base pairing. Among the five UV-treated isolates, we identified 232 SNVs and 2 InDels (Supplemental Dataset S2). The rates of SNVs and InDels were calculated to be 7.9×10^{-9} and 7.0×10^{-11} per base per cell division, respectively (Fig. 1B). These rates represent increases of 124.3-fold and 5.6-fold compared to spontaneous mutation rates. This finding indicates that UV exposure is more likely to stimulate base substitutions than InDels within the *S. spartinae* genome. Among the 232 SNVs identified, 119 were C-to-T/G-to-A transitions, while 60 were T-to-C/A-to-G transitions, constituting the primary types of UV-induced SNVs (Fig. 1B and C). Of the total SNVs, 161 were located in coding regions, including 110 missense variants, 48 synonymous variants, and 3 resulting in stop codons. The relative ratio of intergenic to intragenic SNVs induced by UV exposure did not significantly differ from that of spontaneous SNVs ($P > 0.05$, Chi-square test).

To investigate whether SNVs are influenced by surrounding bases, we extracted trinucleotide sequences with the SNV site positioned in the center from the *S. spartinae* genome. If SNVs are not influenced by adjacent bases, the observed frequency of trinucleotide sequences should approximate the expected frequency based on the genomic context. In the case of spontaneous SNVs, none of the observed frequencies of trinucleotide sequences showed significant enrichment compared to the expected ratios ($P > 0.05$, Chi-square test) (Fig. 3A). In contrast, UV-induced SNVs exhibited a significant context dependency. UV light is known to directly induce lesions and mutations predominantly at pyrimidine sites, meaning that G-to-A substitutions are often indicative of underlying C-to-T substitutions. Figure 3B shows these substitutions in UV-treated cells were more frequently located within the sequences 5'-TCT-3'. Furthermore, the sequence 5'-TTA-3' was notably enriched for UV-induced T-to-C substitutions (Fig. 3B). We also utilized WebLogo 3 to analyze the frequency of adjacent 6-base sequences associated with prominent base substitutions. We observed no significant base enrichment adjacent to the primary spontaneous SNVs (C-to-T substitutions) (Fig. 4A). However, for UV-induced C-to-T substitutions, about 90% of the bases immediately upstream (5') of the SNV site were pyrimidines (Fig. 4B). Specifically, C constituted 34% and T constituted 55% of these bases. This finding leads us to conclude that UV-induced SNVs preferentially occur in pyrimidine-rich regions of the *S. spartinae* genome.

Zeocin exposure led to featured mutations in *S. spartinae*

Zeocin, a member of the bleomycin family, directly binds to DNA and induces various types of lesions, including base oxidation and DNA breaks [30]. This compound has

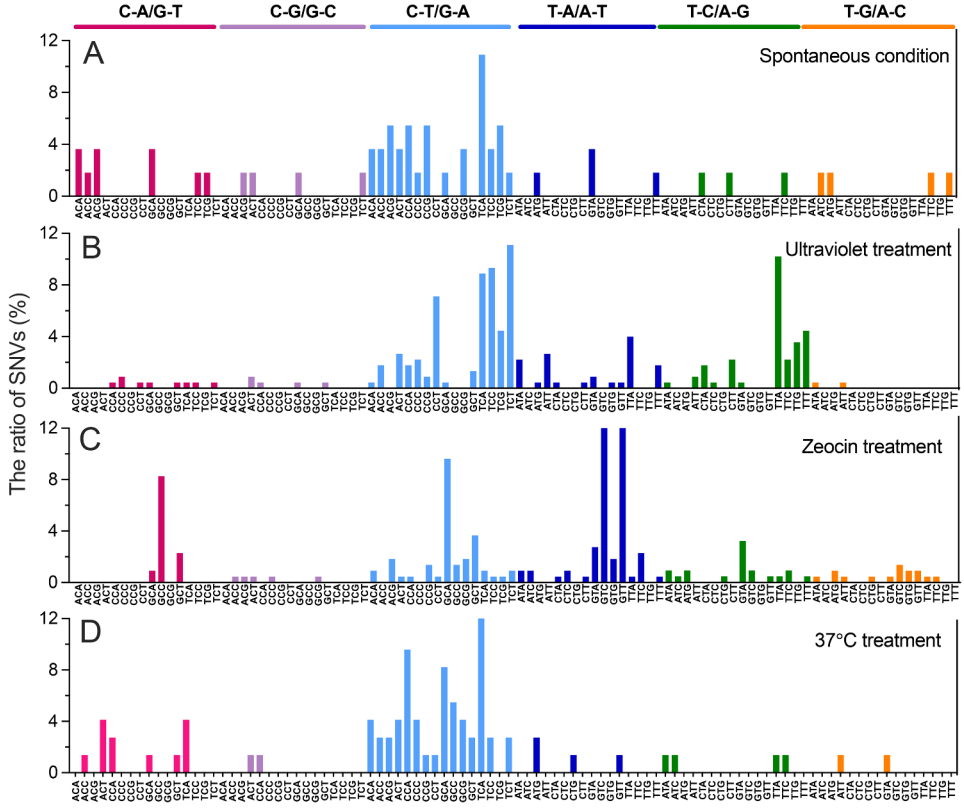

Fig. 3 DNA sequence context of signature mutations. Adjacent sequences of mutated bases under (**A**) spontaneous, (**B**) UV treatment, (**C**) Zeocin treatment, and (**D**) high temperature (37 °C) conditions. SNVs are positioned in the middle of the 3-nucleotide sequences. *P*-values were determined using the Chi-squared test and are indicated with asterisks; * represents $P < 0.05$

been widely utilized as a DNA damage reagent and selection antibiotic in biological studies, as well as a mutagen to enhance the industrial traits of microorganisms [19, 31]. Compared to isolates subcultured under spontaneous conditions, Zeocin-treated isolates exhibited an 80-fold increase in the rates of SNVs (Fig. 1B). Furthermore, the mutation spectrum changed dramatically in the presence of Zeocin, with TA-to-AT (46%) and CG-to-TA (25%) substitutions emerging as the predominant base alterations (Fig. 1C). Previous studies have indicated that the 5′-G-pyrimidine (Py)-3′ motif is particularly susceptible to bleomycin-induced DNA lesions [20, 32]. Consequently, it is likely that most SNVs at A or G sites correspond to mutations occurring at T or C sites on the opposite strand. Assuming all mutations occurred at the T or C sites, we observed that T-to-A substitutions tended to occur at the 5'-GTC-3' and 5'-GTT-3' motifs, while C-to-T substitutions were more frequent at the 5'-GCA-3' sites (Fig. 3C). When considering additional adjacent bases, we identified that the preferred sites for T-to-A substitutions included the 5'-NTGT*YN-3' motif (Y indicates C or T; Fig. 4). These patterns reinforce the notion that Zeocin-induced SNVs in *S. spartinae* adhere to the 5'-G-Py*-3' rule, which describes the specific binding of bleomycin to the 5'-G-T*/C*-3' motif, resulting in damage and mutagenesis of the star-marked pyrimidine.

Compared to UV exposure, Zeocin treatment demonstrated a greater capacity to induce the occurrence of InDels (Fig. 1B). A total of 44 InDels were detected in the Zeocin-treated isolates, with 89% classified as small deletions, indicating that InDels occurred at a rate of 9.6×10^{-10} per base per cell division. In Zeocin-treated *S. cerevisiae* isolates, the predominant class of InDels was identified as transitions from 5'-GT-3' to 5'-G-3', accounting for 63% of all detected InDels [20]. Here, we observed that 10 T deletions occurring at the 5'-GT-3' motifs. These findings suggest that the 5'-GT-3' motifs are also preferred sites for Zeocin-induced InDels in *S. spartinae*. Nevertheless, the relative frequency of such 1-bp deletions at 5'-GT-3' motifs was significantly lower than that observed in *S. cerevisiae* ($P < 0.05$, Fisher's exact test). Annotation of the InDels revealed that 18 of them resulted in frame-shifting variants in *S. spartinae* genes (Supplemental Dataset S3). This result demonstrated that Zeocin can serve as a powerful mutagen to completely deactivate the functions of genes in genetic breeding.

Previous studies have shown that Zeocin treatment can stimulate large deletions and duplications in *S. cerevisiae*,

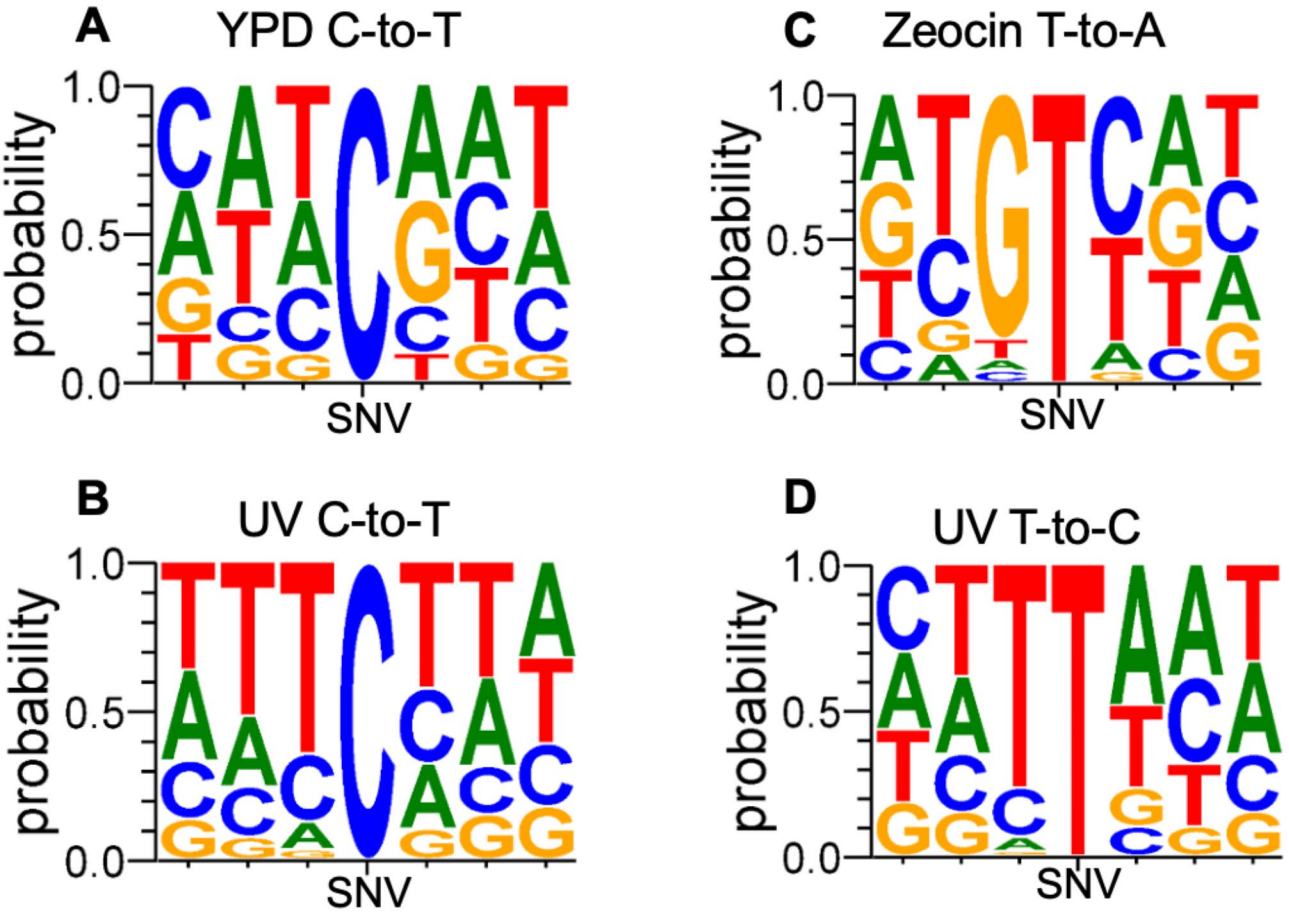

Fig. 4 Identification of preferred DNA motifs for SNVs. Adjacent 6-base sequences for prominent SNVs are presented for the following conditions: (**A**) spontaneous, (**B**) UV treatment, C-to-T (**C**) Zeocin treatment, and (**D**) UV treatment, T-to-C. These sequences were generated using WebLogo 3

with a reported rate of 3.6×10^{-3} events per genome per cell division [20]. However, since we did not detect any large-scale DNA copy number variations in the Zeocin-treated *S. spartinae* isolates, we were unable to calculate their accurate rates. Assuming that one event occurred, the estimated rate of chromosomal rearrangement was calculated to be 1.8×10^{-4} per isolate per cell division. This analysis indicates that chromosomal rearrangements, which typically involve changes in the copy number of numerous genes, are less likely to occur or are less tolerated in the *S. spartinae* genome, whether under spontaneous conditions or in the presence of DNA-damaging agents.

Genomic alterations in *S. spartinae* under heat stress

Anomalous temperature is a common stress factor for microorganisms, both in natural environments and industrial applications. High temperature has been proven to stimulate genome instability and pathogenicity in multiple yeast [21, 33]. To investigate whether elevated temperatures would affect the rates and spectrum of DNA mutations in *S. spartinae*, we subcultured the YMxiao isolates at 37 °C for varying generations. Initially, we sequenced the genomes of 3 strains after 30 generations of subculture, but found very few mutations in their genomes (Dataset S4). Therefore, we extended the propagation to 60 (13 isolates) and 90 (5 isolates) generations for genomic alterations accumulation. The sequencing data revealed a total of 70 SNVs and 39 InDels among these 18 isolates (Dataset S4), resulting in SNV and InDel rates of 9.2×10^{-11} and 5.1×10^{-11} per base pair per cell division, respectively (Fig. 1B). These rates are 1.5- and 3-fold higher than those observed under spontaneous conditions. The prevailing type of base substitution identified was C-to-T or G-to-A, which accounted for up to 70% of all SNVs (Fig. 1B). The sizes of the 39 InDels ranged from 1 bp to 6 bp, with nearly all heat-induced InDels occurring at tandem dinucleotide or trinucleotide repeats (Dataset S4), consistent with observations made at 30 °C. Our findings suggest that high temperatures may stimulate DNA polymerase slippage, leading to an increase in replication errors and misalignments [34].

Similar to the above-mentioned conditions, no single large-scale deletions/duplications or whole-chromosomal

aneuploidy events were detected in the isolates exposed to heat stress. Interestingly, we observed significant alterations in the copy numbers of rDNA repeats between the 30 °C and 37 °C incubation conditions (Fig. 5; $P < 0.05$, Mann-Whitney U test). The average number of rDNA repeats, located at the right end of chromosome H, was 118 in the isolates subcultured at 30 °C, whereas it decreased to 87 at 37 °C (Fig. 5). The copy number of rDNA repeats were not significantly altered by UV and Zeocin treatment (Fig. 5). Our findings suggest that high temperatures may disrupt the DNA replication process, and the reduction in rDNA copies could serve as an adaptive strategy for cells to cope with replication stress.

Discussion

By analyzing isolates of *S. spartinae* YMxiao that were subcultured under various environmental conditions, we uncovered distinct patterns of multiple types of genomic alterations in this species. Our main findings are summarized as follows: (1) The spontaneous rates of SNVs and InDels in the *S. spartinae* genome were determined per base per cell division. Notably, the SNV rate was found to be lower than that observed in *S. cerevisiae*, likely attributable to meiosis-driven purification. (2) UV exposure resulted in a dramatic increase in the SNV rate, which rose by two orders of magnitude, with the majority of mutations identified as C-to-T transitions occurring predominantly in pyrimidine-rich regions of the *S. spartinae* genome. (3) Treatment with Zeocin led to frequent T-to-A mutations and T deletions specifically at the 5'-CGT*YN-3' motifs. (4) Growth at elevated temperatures moderately altered both the DNA mutation rate and the mutation spectrum. (5) Chromosomal rearrangements and aneuploidy were rarely detected in the *S. spartinae* genome; however, significant alterations in rDNA copy numbers were observed under heat stress. The implications of these findings will be discussed in further detail below.

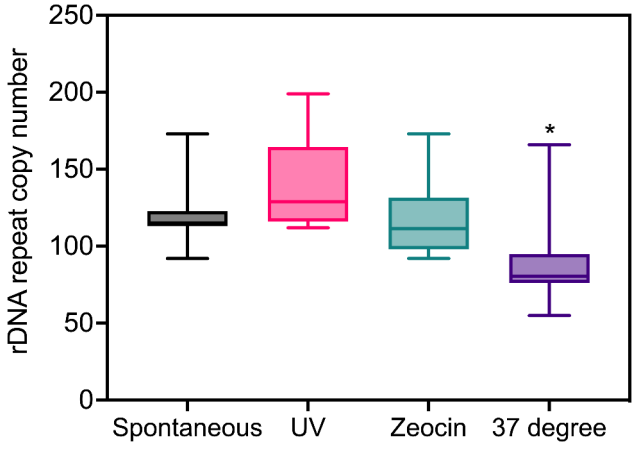

Fig. 5 rDNA copy numbers changes under various conditions. The number of rDNA repeats decreased under heat stress but remained largely unaffected by UV and Zeocin treatments in *S. spartinae* isolates. *P*-values were determined using the Wilcoxon rank-sum test. * represents $P < 0.05$

Under standard growth conditions (YPD medium at 30 °C), the yeast strain *S. spartinae* YMxiao exhibited a lower base substitution rate (6.3×10^{-11} per base pair per cell division) than that observed in diploid *S. cerevisiae* strains. The predominant mutations identified were transitions, specifically cytosine to thymine (C-to-T) and guanine to adenine (G-to-A). These transitions are common in normal metabolic processes and are often attributed to the spontaneous deamination or methylation of cytosine and (Fig. 6A). Interestingly, most SNVs and InDels were found to be homozygous in the diploid *S. spartinae* genome (Dataset S1). This observation contrasts with findings in meiosis-deficient diploid *S. cerevisiae* strains, where the majority of mutations were heterozygous [15]. We hypothesize that the *S. spartinae* isolates underwent meiosis during the subculture process, resulting in the homogenization of nearly all point mutations through meiotic recombination. This purification process likely contributed to a 50% reduction in the observed rates of point mutations. Consequently, we estimate the true rate of SNVs to be approximately 1.3×10^{-10} per base pair per cell division, which aligns more closely with the rates found in *S. cerevisiae* [14, 15, 35]. Stability of production traits is a crucial requirement for industrial microbial strains. The relatively low mutation rate of *S. spartinae*, along with meiosis-driven mutation purification, makes it well-suited to meet this standard. Consistent with findings in other yeast species [15, 36], InDels occurred at a lower rate than SNVs in *S. spartinae*. The primary genetic mechanism driving InDels is template slippage mediated by microsatellites or closely spaced short repeats during DNA replication (Fig. 2B).

Similar to previous observations [16, 37, 38], UV light is also an effective mutagen in *S. spartinae*. Under UV exposure, the prevailing SNVs were C-to-T substitutions (Figs. 1B and 6B). Furthermore, these SNVs frequently occurred with T or C at the 5' position, which aligns with the understanding that the primary DNA lesions caused by UV exposure are cyclobutane pyrimidine dimers (CPDs) [39]. Previous studies in *S. cerevisiae* have emphasized the mutagenic potential of pyrimidine dimers [29, 40, 41]. CPDs pose significant challenges to replicative polymerases, necessitating the involvement of translesion synthesis (TLS) polymerases to bypass these lesions [39, 42]. TLS polymerases are specialized DNA polymerases that allow cells to bypass DNA lesions during replication. Unlike the high-fidelity replicative DNA polymerases, TLS polymerases can replicate over damaged DNA by incorporating nucleotides opposite lesions that would otherwise stall the replication machinery [43, 44]. While this mechanism helps maintain genome

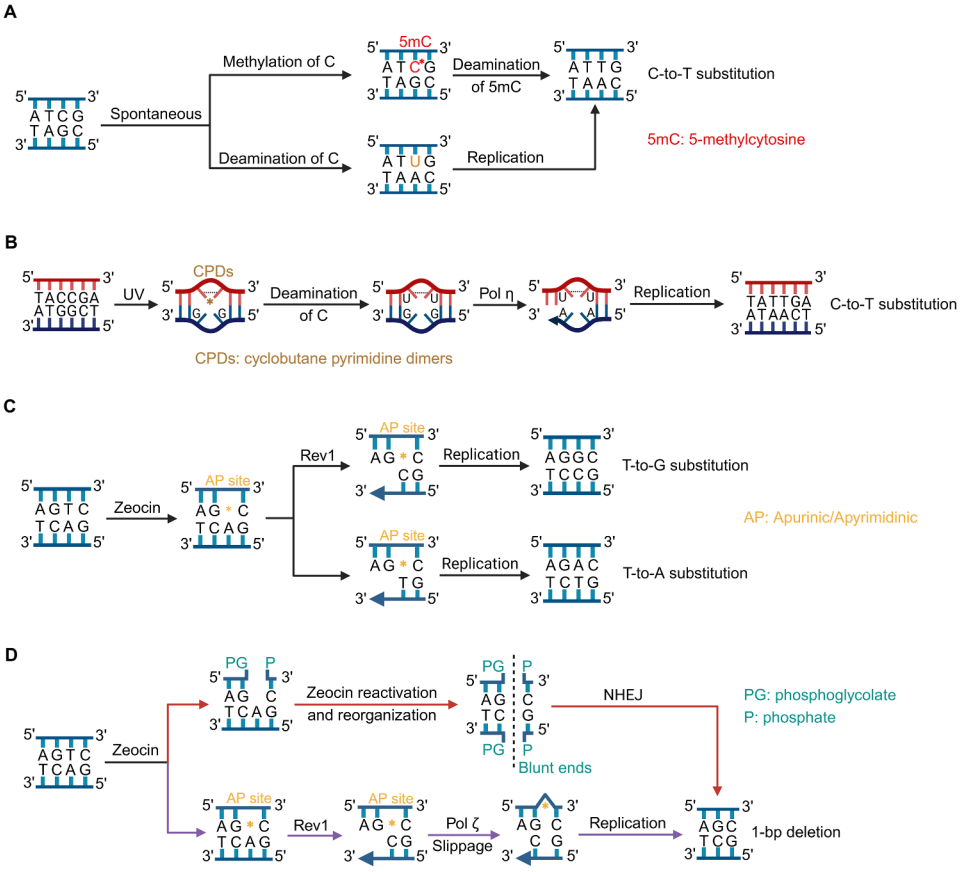

Fig. 6 Genetic models of signature mutations of *S. spartinae* under various conditions. (**A**) C-to-T and G-to-T substitution under spontaneous conditions. (**B**) UV induced C-to-T was associated with CPDs formation. (**C**) Zeocin induced T-to-A and T-to-G were dependent on AP sites formation and translesion synthesis (TLS). (**D**) Two distinct mechanisms underlying Zeocin-induced 1-bp deletion at 5′-GT-3′ motifs

stability by preventing replication fork collapse, it often introduces mutations due to the low fidelity of TLS polymerases. Yeast TLS polymerases include Rev1 (DNA-directed DNA polymerase/deoxycytidyl transferase), ζ, and η [43]. It has been reported that CPDs can act as templates for DNA polymerase η, which facilitates the deamination of cytosine (C to U) within the dimers [45]. This process enables the insertion of adenine opposite the deaminated sites, ultimately leading to C-to-T transitions [45]. It is likely that the UV-induced C-to-T substitutions observed in *S. spartinae* are likely a result of polymerase η dependent bypassing of CPDs. Whether and how the polymerases Rev1 and Pol ζ contribute to UV-induced mutations in *S. spartinae* remain to be determined.

In Zeocin-treated *S. spartinae* isolates, SNVs predominantly occurred at thymine and cytosine bases, consistent with observations in *S. cerevisiae* [20]. However, the relative ratios of base substitutions differed between the two species. In *S. cerevisiae*, the most common SNVs at thymine bases are T-to-G substitutions, accounting for up to 43% of all SNVs [46, 47]. This pattern is likely due to the activity of the error-prone DNA polymerase Rev1, which preferentially incorporates C opposite AP sites, followed by extension by DNA polymerase ζ (Fig. 6C) [46, 47]. Interestingly, in Zeocin-treated *S. spartinae* isolates, T-to-A substitutions were 11.4-fold higher rate than T-to-G substitutions, although both substitutions followed the 5′-GT*-3′ rule. This discrepancy may be due to a unique preference in *S. spartinae* Rev1 (encodes by g4827.t1) for incorporating T rather than C opposite AP sites (Fig. 6C). Zeocin treatment also resulted in a significant increase in InDels, with a notable prevalence of 1-bp deletions (up to 66% of all InDels; Dataset S3). As shown in Fig. 6D, bleomycin is known to create blunt-ended DSBs, and the nonhomologous end joining pathway (NHEJ)'s repair of these breaks can result in 1-bp deletions (Fig. 6D). NHEJ is conserved in many eukaryotes, including yeasts. This pathway operates independently of a homologous template, making it particularly important in the G1 phase of the cell cycle when sister chromatids are unavailable. While efficient, NHEJ is prone to errors and may result in small insertions or deletions at the repair site, potentially leading to mutations [48]. Our results emphasize that the diverse functions and activities of error-prone DNA polymerases and the NHEJ pathway

are crucial for modifying Zeocin-induced mutation patterns in different yeast strains.

Previous studies have shown that heat stress can destabilize the replication machinery, leading to an increase in DNA replication errors [49]. Elevated temperatures also enhance metabolic rates, resulting in increased production of reactive oxygen species, which can cause oxidative DNA damage, such as the formation of 8-oxoguanine. In our findings, we observed that DNA mutations in *S. spartinae* were elevated at higher incubation temperatures, although the inductive effect was considerably weaker compared to that observed under UV and Zeocin treatments. Notably, at elevated temperatures, InDels were more likely to be triggered than SNVs. This observation may indicate that template slippage occurs more frequently under heat stress, potentially due to the reduced processivity of DNA polymerases. Alternatively, the activity of the mismatch repair pathway—which corrects mismatched errors introduced by DNA polymerases to prevent InDels—may be inhibited at higher temperatures.

Chromosomal rearrangements, including large deletions, duplications, translocations, and inversions, are commonly observed in certain yeast species, such as *S. cerevisiae* and *Candida albicans* [11, 50]. These genetic events occur at an approximate rate of 10^{-4} per cell division, facilitating rapid phenotypic evolution in *S. cerevisiae* [15]. However, despite the significant induction of DNA breaks and recombination by UV and Zeocin treatments [19, 51], no chromosomal recombination events affecting gene copy numbers were detected in the *S. spartinae* isolates. In contrast, we observed a significant decrease in rDNA copy numbers under heat stress, while no such changes occurred under UV or Zeocin treatments (Fig. 5). In cells, rDNA is crucial for ribosome biogenesis and protein synthesis. The rDNA region typically exists as tandem repeats, and its copy number can vary based on species and environmental conditions [52]. Our previous studies indicated that yeast cells experiencing DNA replication stress, characterized by the downregulation of DNA polymerases, exhibited reduced rDNA repeat copy numbers. This reduction may alleviate replication burden and promote cell growth [53, 54]. A similar phenomenon has been observed in cancer cells, where replication stress is a common hallmark [55]. Thus, we hypothesize that elevated temperatures may induce cumulative DNA replication stress, with rDNA instability serving as an adaptive mechanism for *S. spartinae* to mitigate heat stress. The plasticity of rDNA copy number may not only enhance the survival of this species under environmental challenges, such as temperature fluctuations and nutrient limitations in natural settings, but also confer potential advantages in industrial applications. For instance, during industrial fermentation in tropical climates or during summer, substantial energy input is required for cooling to maintain optimal process conditions [56]. The development of thermotolerant yeast strains could mitigate the energy demands associated with cooling systems, thereby enhancing the overall efficiency and sustainability of industrial fermentation processes [56]. Whether rDNA instability can be detected in other yeast species under high-temperature conditions warrants further investigation.

Conclusions

This study elucidated the genomic alterations in *S. spartinae* under optimal growth and mutagenic conditions. We found that UV radiation, Zeocin treatment, and elevated temperatures significantly increased mutation rates and altered the mutation spectrum in this yeast. Both spontaneous and induced mutations were found to be homozygous in the *S. spartinae* genome, likely due to meiosis-driven purification. Changes in rDNA copy number are likely a genetic strategy for rapid adaptability of *S. spartinae* under various stressors, including heat. Unlike *S. cerevisiae*, *S. spartinae* is highly sensitive to abnormalities that alter DNA copy number. The lower rates of DNA mutations and copy number variations in non-rDNA regions of *S. spartinae* may help preserve consistent production traits, making it advantageous for industrial applications. Notably, our results emphasized that different mutagenic conditions lead to distinct sequence context-dependent mutations, highlighting the specific interactions between various mutagens and DNA. These findings provide new insights into the genomic plasticity of yeasts and enhance our understanding of their genetic adaptive mechanisms in diverse environments.

Abbreviations

MA	Mutation accumulation
SNVs	Single nucleotide variations
InDels	Insertions and deletions
LOH	Loss of heterozygosity
UV	Ultraviolet
gDNA	Genomic DNA
CPDs	Cyclobutane pyrimidine dimers
TLS	Translesion synthesis
NHEJ	Nonhomologous end joining pathway

Supplementary Information

The online version contains supplementary material available at https://doi.org/10.1186/s12864-025-11479-z.

Supplementary Material 1

Supplementary Material 2

Acknowledgements

We thank the comments from the members from DQ's lab to improve this manuscript.

Author contributions
Y.T.B. and A.S. conducted the experiments. Q.X., L.Y.T., and K.J.L. performed the data analysis. B.Y.G. provided suggestions for revising the initial draft. L.Q. and D.Q.Z. prepared the figures and completed the drafting and revision of the manuscript. All authors contributed to the final revisions of the manuscript.

Funding
This study was supported by the National Key R&D Program of China (2023YFE0124700), the Fundamental Research Funds for the Central Universities (226-2024-00019), the Key Research and Development Program of Hainan Province (ZDYF2024SHFZ046), and the National Natural Science Foundation of Zhejiang Province (LDT23D06022D06).

Data availability
The telomere-to-telomere genome sequence of ***S. spartinae*** YMxiao was assembled in our previous study and being available from DDBJ/ENA/GenBank with the accession JBJABQ000000000. The raw data of whole genome sequencing of ***S. spartinae*** YMxiao isolates were deposited in SRA database with the accession number of PRJNA1187357.

Declarations

Ethical approval
This study does not describe any experimental work related to humans.

Conflict of interest
The authors declare that there are no conflicts of interest.

Consent for publication
Not applicable.

Received: 23 November 2024 / Accepted: 12 March 2025
Published online: 25 March 2025

References

1. Onyema V, Amadi O, Moneke A, Agu R. A brief review: *Saccharomyces cerevisiae* biodiversity potential and promising cell factories for exploitation in biotechnology and industry processes–west African natural yeasts contribution. Food Chem Adv. 2023;2:100162.
2. Duina AA, Miller ME, Keeney JB. Budding yeast for budding geneticists: a primer on the *Saccharomyces cerevisiae* model system. Genetics. 2014;197(1):33–48.
3. Chi Z, Liu G-L, Lu Y, Jiang H, Chi Z-M. Bio-products produced by marine yeasts and their potential applications. Bioresour Technol. 2016;202:244–52.
4. Ahmed FK, Kalia A, Ahmad A, Alghuthaymi MA, Abd-Elsalam KA. Marine fungi and yeast: A green approach for production of bionanoparticles. Fungal cell factories for sustainable nanomaterials productions and agricultural applications. Elsevier; 2023. pp. 337–60.
5. Abdel-Mawgoud AM, Markham KA, Palmer CM, Liu N, Stephanopoulos G, Alper HS. Metabolic engineering in the host *Yarrowia lipolytica*. Metab Eng. 2018;50:192–208.
6. Miller KK, Alper HS. *Yarrowia lipolytica*: more than an oleaginous workhorse. Appl Microbiol Biotechnol. 2019;103(23–24):9251–62.
7. Liu HH, Ji XJ, Huang H. Biotechnological applications of *Yarrowia lipolytica*: past, present and future. Biotechnol Adv. 2015;33(8):1522–46.
8. Tan L, He M, Song L, Fu X, Shi SJBT. Aerobic decolorization, degradation and detoxification of Azo dyes by a newly isolated salt-tolerant yeast *Scheffersomyces spartinae* TLHS-SF1. Bioresour Technol. 2016;203:287–94.
9. Song L, Shao Y, Ning S, Tan LJB. Performance of a newly isolated salt-tolerant yeast strain Pichia occidentalis G1 for degrading and detoxifying Azo dyes. Bioresour Technol. 2017;233:21–9.
10. Sharma A, Liu X, Yin J, Yu PJ, Qi L, He M, Li KJ, Zheng DQ. Genomic characteristics and genetic manipulation of the marine yeast. Appl Microbiol Biotechnol 2024, 108(1).
11. Li K-J, Qi L, Zhu Y-X, He M, Xiang Q, Zheng D-Q. Spontaneous and environment induced genomic alterations in yeast model. Cell Insight 2024:100209.
12. Hanway D, Chin JK, Xia G, Oshiro G, Winzeler EA, Romesberg FE. Previously uncharacterized genes in the UV-and MMS-induced DNA damage response in yeast. Proc Natl Acad Sci U S A. 2002;99(16):10605–10.
13. Zhu YO, Siegal ML, Hall DW, Petrov DA. Precise estimates of mutation rate and spectrum in yeast. Proc Natl Acad Sci U S A. 2014;111(22):E2310–8.
14. Sampaio NM, Ajith V, Watson RA, Heasley LR, Chakraborty P, Rodrigues-Prause A, Malc EP, Mieczkowski PA, Nishant KT, Argueso JL. Characterization of systemic genomic instability in budding yeast. Proc Natl Acad Sci U S A. 2020;117(45):28221–31.
15. Sui Y, Qi L, Wu JK, Wen XP, Tang XX, Ma ZJ, Wu XC, Zhang K, Kokoska RJ, Zheng DQ, et al. Genome-wide mapping of spontaneous genetic alterations in diploid yeast cells. Proc Natl Acad Sci U S A. 2020;117(45):28191–200.
16. Yin Y, Petes TD. Genome-wide high-resolution mapping of UV-induced mitotic recombination events in *Saccharomyces cerevisiae*. PLoS Genet. 2013;9(10):e1003894.
17. Barbour L, Hanna M, Xiao W. Mutagenesis. Methods Mol Biol. 2006;313:121–7.
18. Sugiyama T, Keinard B, Best G, Sanyal MR. Biochemical and photochemical mechanisms that produce different UV-induced mutation spectra. Mutat Res. 2021;823:111762.
19. Sheng H, Qi L, Sui Y, Li YZ, Yu LZ, Zhang K, Xu JZ, Wang PM, Zheng DQ. Mapping chromosomal instability induced by small-molecular therapeutics in a yeast model. Appl Microbiol Biot. 2019;103(12):4869–80.
20. Zheng DQ, Wang YT, Zhu YX, Sheng H, Li KJ, Sui Y, Zhang K. Uncovering bleomycin-induced genomic alterations and underlying mechanisms in the yeast *Saccharomyces cerevisiae*. Appl Environ Microbiol. 2022;88(2):e0170321.
21. Shen L, Wang Y-T, Tang X-X, Zhang K, Wang P-M, Sui Y, Zheng D-Q. Heat shock drives genomic instability and phenotypic variations in yeast. AMB Express. 2020;10(1):1–11.
22. Zhang K, Zheng DQ, Sui Y, Qi L, Petes TD. Genome-wide analysis of genomic alterations induced by oxidative DNA damage in yeast. Nucleic Acids Res. 2019;47(7):3521–35.
23. Qi L, Zhang K, Wang YT, Wu JK, Sui Y, Liang XZ, Yu LZ, Wu XC, Wang PM, Xu JZ et al. Global analysis of furfural-induced genomic instability using a yeast model. Appl Environ Microbiol 2019, 85(18).
24. Qi L, Zhu YX, Wang YK, Tang XX, Li KJ, He M, Sui Y, Wang PM, Zheng DQ, Zhang K. Nonlethal furfural exposure causes genomic alterations and adaptability evolution in *Saccharomyces cerevisiae*. Microbiol Spectr. 2023;11(4):e0121623.
25. Zhu Y-X, He M, Li K-J, Wang Y-K, Qian N, Wang Z-F, Sheng H, Sui Y, Zhang D-D, Zhang K. Novel insights into the effects of 5-hydroxymethfurural on genomic instability and phenotypic evolution using a yeast model. Appl Environ Microbiol. 2024;90(1):e01649–01623.
26. Li H, Durbin R. Fast and accurate short read alignment with Burrows-Wheeler transform. Bioinformatics. 2009;25(14):1754–60.
27. Quinlan AR, Hall IM. BEDTools: a flexible suite of utilities for comparing genomic features. Bioinformatics. 2010;26(6):841–2.
28. Dong YT, Miao RY, Feng RC, Wang T, Yan JJ, Zhao X, Han X, Gan Y, Lin JB, Li YJ, et al. Edible and medicinal fungi breeding techniques, a review: current status and future prospects. Curr Res Food Sci. 2022;5:2070–80.
29. Brash DEJP. Photobiology: UV signature mutations. Photochem Photobiol. 2015;91(1):15–26.
30. Bolzán AD, Bianchi MS. DNA and chromosome damage induced by bleomycin in mammalian cells: an update. Mutat Res Rev Mutat Res. 2018;775:51–62.
31. Zhao B, Li YF, Li CL, Yang HL, Wang W. Enhancement of *Schizochytrium* DHA synthesis by plasma mutagenesis aided with malonic acid and Zeocin screening. Appl Microbiol Biot. 2018;102(5):2351–61.
32. Chen J, Stubbe J. Bleomycins: towards better therapeutics. Nat Rev Cancer. 2005;5(2):102–12.
33. Gusa A, Yadav V, Roth C, Williams JD, Shouse EM, Magwene P, Heitman J, Jinks-Robertson S. Genome-wide analysis of heat stress-stimulated transposon mobility in the human fungal pathogen *Cryptococcus deneoformans*. Proc Natl Acad Sci U S A. 2023;120(4):e2209831120.
34. Gasch AP, Spellman PT, Kao CM, Carmel-Harel O, Eisen MB, Storz G, Botstein D. Brown POJMbotc: genomic expression programs in the response of yeast cells to environmental changes. Mol Biol Cell. 2000;11(12):4241–57.
35. Loeillet S, Herzog M, Puddu F, Legoix P, Baulande S, Jackson SP, Nicolas AG. Trajectory and uniqueness of mutational signatures in yeast mutators. Proc Natl Acad Sci U S A. 2020;117(40):24947–56.
36. Dutta A, Dutreux F, Schacherer J. Loss of heterozygosity spectrum depends on ploidy level in natural yeast populations. Mol Biol Evol. 2022;39(11):msac214.
37. Narayanan DL, Saladi RN, Fox JL. Ultraviolet radiation and skin cancer. Int J Dermatol. 2010;49(9):978–86.

38. Alves RN, Agustí S. Oxidative stress in tissues of Gilthead seabream (Sparus aurata) and European Seabass (Dicentrarchus labrax) juveniles exposed to ultraviolet-B radiation. J Photochem Photobiol. 2021;8:100070.
39. Waters LS, Minesinger BK, Wiltrout ME, D'Souza S, Woodruff RV, Walker GC. Eukaryotic translesion polymerases and their roles and regulation in DNA damage tolerance. Microbiol Mol Biol Rev. 2009;73(1):134–54.
40. Alexandrov LB, Kim J, Haradhvala NJ, Huang MN, Tian Ng AW, Wu Y, Boot A, Covington KR, Gordenin DA, Bergstrom EN, et al. The repertoire of mutational signatures in human cancer. Nature. 2020;578(7793):94–101.
41. Brash DE. UV signature mutations. Photochem Photobiol. 2015;91(1):15–26.
42. Maiorano D, El Etri J, Franchet C, Hoffmann JS. Translesion synthesis or repair by specialized DNA polymerases limits excessive genomic instability upon replication stress. Int J Mol Sci 2021, 22(8).
43. Makarova AV, Burgers PM. Eukaryotic DNA polymerase Z. DNA Repair (Amst). 2015;29:47–55.
44. Goodman MF, Woodgate R. Translesion DNA polymerases. Cold Spring Harb Perspect Biol 2013, 5(10).
45. Menck CFM, Galhardo RS, Quinet A. The accurate bypass of pyrimidine dimers by DNA polymerase Eta contributes to ultraviolet-induced mutagenesis. Mutat Res. 2024;828:111840.
46. McIntyre J. Polymerase iota - an odd sibling among Y family polymerases. DNA Repair (Amst). 2020;86:102753.
47. Jiang G, Wang J, Zhao D, Chen X, Pu S, Zhang C, Li J, Li Y, Yang J, Li S, et al. Molecular mechanism of the cytosine CRISPR base editing process and the roles of translesion DNA polymerases. ACS Synth Biol. 2021;10(12):3353–8.
48. Rodgers K, McVey M. Error-Prone repair of DNA Double-Strand breaks. J Cell Physiol. 2016;231(1):15–24.
49. Aguilera A, García-Muse, TJArog. Causes of genome instability. Annu Rev Genet. 2013;47(1):1–32.
50. Oggenfuss U, Todd RT, Soisangwan N, Kemp B, Guyer A, Beach A, Selmecki A. *Candida albicans* isolates contain frequent heterozygous structural variants and transposable elements within genes and centromeres. *Genome Res* 2024:gr. 279301.279124.
51. Yin Y, Dominska M, Yim E, Petes TD. High-resolution mapping of heteroduplex DNA formed during UV-induced and spontaneous mitotic recombination events in yeast. Elife. 2017;6:e28069.
52. Hori Y, Engel C, Kobayashi T. Regulation of ribosomal RNA gene copy number, transcription and nucleolus organization in eukaryotes. Nat Rev Mol Cell Biol. 2023;24(6):414–29.
53. Zheng DQ, Zhang K, Wu XC, Mieczkowski PA, Petes TD. Global analysis of genomic instability caused by DNA replication stress in *Saccharomyces cerevisiae*. Proc Natl Acad Sci U S A. 2016;113(50):E8114–21.
54. Zhang K, Sui Y, Li W-L, Chen G, Wu X-C, Kokoska RJ, Petes TD, Zheng D-Q. Global genomic instability caused by reduced expression of DNA polymerase ε in yeast. Proc Natl Acad Sci U S A. 2022;119(12):e2119588119.
55. Xu B, Li H, Perry JM, Singh VP, Unruh J, Yu Z, Zakari M, McDowell W, Li L, Gerton JL. Ribosomal DNA copy number loss and sequence variation in cancer. PLoS Genet. 2017;13(6):e1006771.
56. Abdel-Banat BMA, Hoshida H, Ano A, Nonklang S, Akada R. High-temperature fermentation: how can processes for ethanol production at high temperatures become superior to the traditional process using mesophilic yeast? Appl Microbiol Biot. 2010;85(4):861–7.

Publisher's note